

# Autonomous bottom-up fabrication of three-dimensional nano/microcellulose honeycomb structures, directed by bacterial nanobuilder

Tetsuo Kondo\* and Wakako Kasai

Graduate School of Bioresource and Bioenvironmental Sciences, Kyushu University, 6-10-1 Hakozaki, Higashi-ku, Fukuoka 812-8581, Japan

Received 10 January 2014; accepted 2 April 2014

Available online 3 May 2014

**We investigated the autonomous bottom-up fabrication of three-dimensional honeycomb cellulose structures, using *Gluconacetobacter xylinus* as a bacterial nanoengine, on cellulose honeycomb templates prepared by casting water-in-oil emulsions on glass substrates (Kasai and Kondo, *Macromol. Biosci.*, 4, 17–21, 2004). The template film had a unique molecular orientation state along the honeycomb frames, but was non-crystalline. When *G. xylinus*, used as a nanofiber-producing bacterium, was incubated on the honeycomb scaffold in a culture medium, it secreted cellulose nanofibers only on the upper surface of the honeycomb frame. The movement was regulated by a selective interaction between the synthesized nanofiber and the surface of the honeycomb frames of the template. The relationship between directed deposition of synthesized nanofibers and ordered fabrication from the nano- to the micro-scale could provide a novel bottom-up methodology, using bacteria, for the design of three-dimensional honeycomb structures as functional materials with nano/micro hierarchical structures, with low energy consumption.**

© 2014, The Society for Biotechnology, Japan. All rights reserved.

**[Key words:** *Gluconacetobacter xylinus*; Directed three-dimensional nano/micropatterning; Cellulose; Nanofiber; Autonomous fabrication; Honeycomb scaffold; Bacterial nanoengine]

During cellulose synthesis, *Gluconacetobacter xylinus* (formerly *Acetobacter xylinum*), a gram-negative bacterium, moves at a rate of 2.0  $\mu\text{m}/\text{min}$  at 25°C, as a result of an inverse force derived from the secretion of crystalline cellulose microfibrils of width 3–4 nm (1). The secreted microfibrils then self-assemble to give nanofibers, called cellulose ribbons, with an average width of 50 nm and thickness of 10 nm.

We recently found that *G. xylinus* cells, which synthesize and extrude cellulose microfibril bundles, direct epitaxial deposition of nanofibers along the molecular tracks on nematic ordered cellulose (NOC) (2–4) templates, which are highly ordered but not crystalline (5,6). NOC has unique characteristics; in particular, its surface properties provide tracks or scaffolds for regulation of the movement and fiber production direction of *G. xylinus*. This is because the interactions between the produced microbial cellulose nanofibers and specific sites on the oriented molecules on the NOC are very strong. These ordered cellulose substrates can be used as templates for the construction of nanocomposites, and the growth direction of the secreted cellulose is controlled by the epitaxial deposition of the microfibrils. Accordingly, the template could be used as a scaffold to regulate the NOC-patterned three-dimensional (3D) architecture of cellulose-ribbon-like nanofibers by incubating bacteria on the template.

We also investigated the transfer of active *G. xylinus* cells to nematic ordered chitin surfaces instead of NOC, and found that the synthesized cellulose nanofibers (i.e., cellulose ribbons) were not

parallel to the molecular orientation of the substrate, unlike the secreted fibers deposited on NOC templates. The bacteria initially followed the molecular tracks, but soon repeatedly jumped off the tracks and synthesized cellulose parallel to neighboring tracks. This wavy pattern was repeated across the template (6,7). These results indicated that adhesion for epitaxial growth of deposited microfibrils depends on several critical factors related to the molecular order of the substrate. This order is represented by three factors: the molecular chain orientation, specific polymer chain conformation, and O6 rotational position with respect to O5 and C4 in the  $\beta$ -glucan chain. The importance of the molecular chain orientation was supported by the observation that unstretched NOC does not cause epitaxial deposition (6).

NOC is prepared by uniaxial stretching of a water-swollen cellulose gel from *N,N*-dimethylacetamide/LiCl solution (2,3), and the cellulose molecular chains tend to be oriented along the stretching axis. Cellulose has an extended structure with a 2<sub>1</sub> screw axis composed of  $\beta$ -1,4-glucosidic linkages between anhydroglucose units; all the hydroxyl groups are bonded to glucose rings equatorially, whereas the CH groups are axially bonded to glucose rings. On the NOC surface, hydrophobic and hydrophilic sites tend to be aligned alternately, like tracks, along the stretching axis, because the glucopyranose rings are slightly tilted towards the surface (3–6). This pattern induces strong interactions between the ordered molecules of the template and species such as fibers (4–6) and organic and inorganic molecules (8). The constant rate of bacterial cell movement along the ordered molecules of the NOC template scaffold is 4.5  $\mu\text{m}/\text{min}$  at 24°C; this is faster than normal cell movements (1,5). These observations show that the bacteria follow patterns based on the template characteristics if the secreted

\* Corresponding author. Tel./fax: +81 92 642 2997.

E-mail address: [tekondo@agr.kyushu-u.ac.jp](mailto:tekondo@agr.kyushu-u.ac.jp) (T. Kondo).

fibers can interact strongly with the surface of a template similar to NOC.

Kasai and Kondo explored other types of templates (9) and reported the first successful fabrication of cellulose and cellulose acetate films with honeycomb-patterned pores. These were produced by casting water-in-oil emulsions on glass substrates in a saturated water vapor atmosphere. Micropatterned honeycomb films are formed more easily using this technique than by using lithographic techniques such as photolithography. In the film preparation, a honeycomb-patterned cellulose acetate was fabricated and then deacetylated to yield a cellulose film, without deformation of the honeycomb pores; the micropore sizes ranged from 1 to 100  $\mu\text{m}$ , depending on the preparation conditions. As the volatile solvent in the polymer solution evaporated, the polymer precipitated to form a film, which simultaneously caused stretching by natural drying. The honeycomb-patterned frames are therefore expected to have specific arrangements of  $\beta$ -glucan chains, based on the NOC, which functions as a template.

In the present study, we performed detailed characterizations of the super- and supra-molecular structures of these honeycomb-patterned films, using polarized light microscopy and X-ray diffraction analyses. The ordered structure of the  $\beta$ -glucan molecules in the film as a result of the stretching effect during natural drying was elucidated. Moreover, the obtained honeycomb film was used as a template for autonomous bottom-up fabrication of 3D honeycomb structures at the nano/microscales by regulated movements of bacteria on the honeycomb-patterned frames.

#### MATERIALS AND METHODS

**Materials** Cellulose triacetate (80–110 cP) provided by Wako Pure Chemical Industries Ltd. (Osaka, Japan) was used as the starting material for fabricating honeycomb-patterned cellulose films. The water used was purified using a NANO-pure Diamond Ultrapure Water System (Barnstead International, Dubuque, IA, USA). All solvents were reagent grade and were used without further purification.

**Preparation and characterization of honeycomb-patterned films** Honeycomb-patterned films were prepared as described in our previous report (9). Polarized microscopic images were observed using a transmission optical microscope equipped with a polarizing system (Leica DMRE; Leica Microsystems Inc., Wetzlar, Germany) to examine the orientations of the molecular chains in the honeycomb frames. Frame birefringence was examined using a Zeiss polarized microscope (Carl Zeiss Microscopy GmbH, Jena, Germany) with a compensator.

The crystallinities of the honeycomb-patterned films were determined with a Rigaku RINT Ultima III X-ray generator (Rigaku Co., Tokyo, Japan) using Ni-filtered

CuK $\alpha$  radiation produced at 40 kV and 50 mA. The scanning rate was 2°/min and the 2 $\theta$  range was 3°–60°.

**Autonomous bottom-up fabrication of 3D nano/microcellulose honeycomb structures** A honeycomb-patterned cellulose film was fixed on a glass slide, and the slide was placed in Schramm–Hestrin (SH) medium (10) at pH 6.0, and kept in a Petri dish until use.

*G. xylinus* (NQ-5; ATCC53582) was cultured in SH medium containing cellulase ONOZUKA R-10 (Yakult Pharmaceutical Industry Co., Ltd., Tokyo, Japan) at pH 6.0 to obtain the active bacteria. After cultivation for 3 d, the medium was filtered using a nylon mesh with pores of diameter 40  $\mu\text{m}$ . The medium was then changed to the normal SH medium, using centrifugation to remove the cellulase. The bacteria were then incubated in the same SH medium in an Erlenmeyer flask, which was fixed to a valuable rotator, and the flask was kept under rotation at 20 rpm to allow them to selectively attach to the surfaces of the honeycomb frames in the template scaffold.

**Measurements and analyses** Real-time video analyses were performed using light microscopic images acquired with a  $\times 50$  objective lens, coupled with a  $\times 1.25$  Optivar lens, using a Leica light microscope (Leica DMRE; Leica Microsystems) equipped with a color chilled three-charge-coupled device camera (C5810; Hamamatsu Photonics K.K., Shizuoka, Japan), with a  $\times 0.55$  camera lens (HR 055-CMT; Diagnostic Instruments Inc., Sterling Heights, MI, USA). Each frame was captured, digitized, saved, and processed using Image Pro Plus 4.1 (Media Cybernetics, Inc., Rockville, MD, USA) at an acquisition rate of one frame every 20 s (three frames per minute). The observed images were specimens of the bacteria on the substrates, covered with SH medium kept just above the surface at 24°C. The focus of the camera was set between the bacteria and the substrate surface so that the bacteria and the synthesized cellulose nanofibers could both be observed. The incident light in the system was minimized to prevent drying of the surface by the heat produced. Adobe PREMIER 6.0 was used to sequence the captured frames to produce a movie, at a rate of 30 frames per second.

The topographic features of the films were also determined using atomic force microscopy (AFM; Nanopics 2100; Seiko Instruments Inc., Chiba, Japan). The observations were performed in air at room temperature, in damping mode, with a scan rate of 1–2 line/s, to obtain 200  $\times$  200  $\mu\text{m}^2$  areas. The AFM tip was a commercial Si tip, with a nominal radius less than 20 nm. The spring constant of the cantilever was 40 N/m (DFMPC120, provided by Seiko Instruments Inc.).

#### RESULTS AND DISCUSSION

**Characterization of honeycomb-patterned cellulose triacetate and cellulose films** The orientations of the cellulose molecular chains in honeycomb-patterned cellulose triacetate films were examined using a polarized microscope equipped with a compensator, as shown in Fig. 1. The interference color shifts from yellow to blue on rotating the specimen through 90° (Fig. 1C and D). When the yellow color of the specimen is perpendicular to the Z-axis of the compensator, the molecular orientation within the honeycomb structure is perpendicular to the Z-axis (Fig. 1C, white

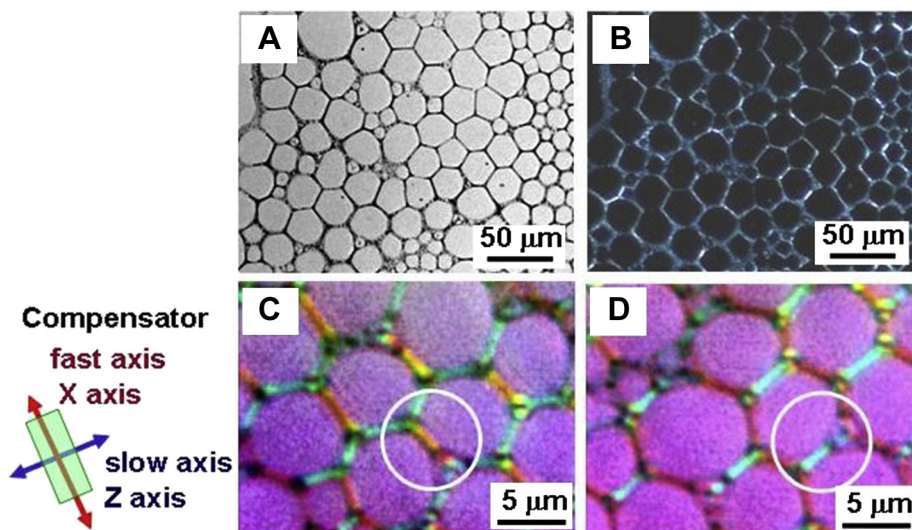


FIG. 1. Micrographs of honeycomb-patterned film from cellulose triacetate. Images were observed in (A) bright field, (B) polarized mode, (C) polarized mode with a compensator rotating the film at 0°, and (D) polarized mode with a compensator rotating the film at 90°. (C, D) White circle areas show identical frames.

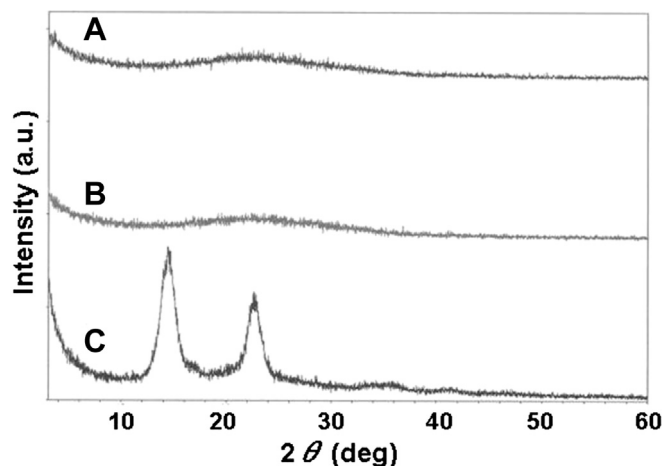


FIG. 2. X-ray diffractograms of honeycomb-patterned films: (A) cellulose film, (B) cellulose triacetate film, and (C) microbial cellulose film (pellicle) from *Gluconacetobacter xylinus* as a reference.

circle). Blue indicates that the molecular orientation is parallel to the Z-axis of the compensator (Fig. 1D, white circle). A honeycomb-patterned cellulose film exhibited the same features (not shown here). These results indicated that the honeycomb frames of the cellulose and cellulose acetate films were both molecularly well aligned to the direction of each honeycomb frame. This is probably the result of stretching by natural drying

of the honeycomb-patterned frames in the presence of water droplets as molds, as mentioned above.

The crystallinities of cellulose and cellulose triacetate films with honeycomb patterns were investigated using reflection-mode X-ray diffraction. Fig. 2 shows the X-ray diffractograms of both the honeycomb-patterned films and of a microbial cellulose film (dried pellicle secreted from *G. xylinus*) as a reference. Diffuse patterns, arising from non-crystalline regions, were seen in the X-ray patterns of both the honeycomb films, indicating that both films had no or low crystallinity, although these diffuse patterns might also be caused by the low densities of the films as a result of the honeycomb structures. Solubility tests were therefore performed to further examine the crystallinities.

The solubilities of the honeycomb-patterned cellulose films had an interesting feature: they were easily dissolved in 7% NaOH aqueous solution, whereas conventional cellulose films with partially crystalline domains are usually difficult to dissolve in mild alkaline solutions. The solubility tests therefore indirectly proved that the honeycomb-patterned cellulose and cellulose triacetate films were non-crystalline, even though the molecular chains in the honeycomb frames were well ordered, as described above. The results suggested that the film structures were similar to those of NOC and chitin, which are well oriented but not highly crystalline, as previously reported (2–4,6,11).

**Autonomous bottom-up fabrication of 3D nano/microcellulose honeycomb structures produced using *G. xylinus* cells** A honeycomb-patterned cellulose film was used as a scaffold for the culture of *G. xylinus*, which secretes

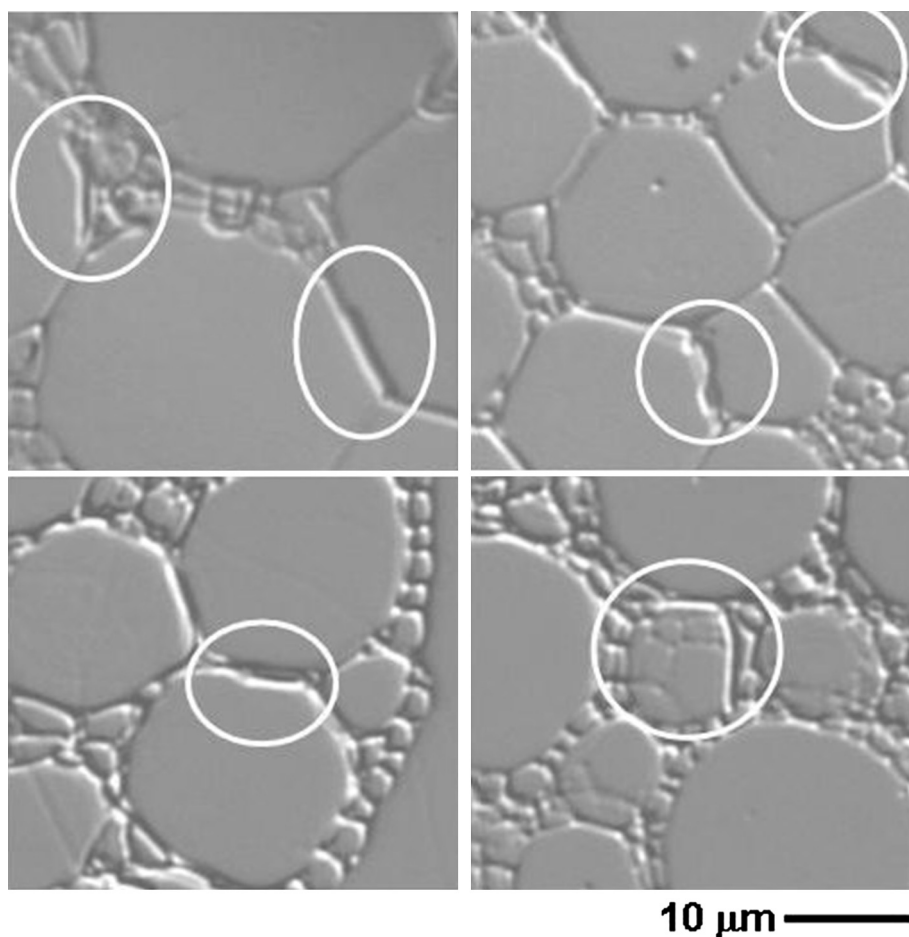


FIG. 3. Differential interference light microscopic images of selective attachment of bacteria (inside circles) on surfaces of honeycomb frames under slow rotation during culture.

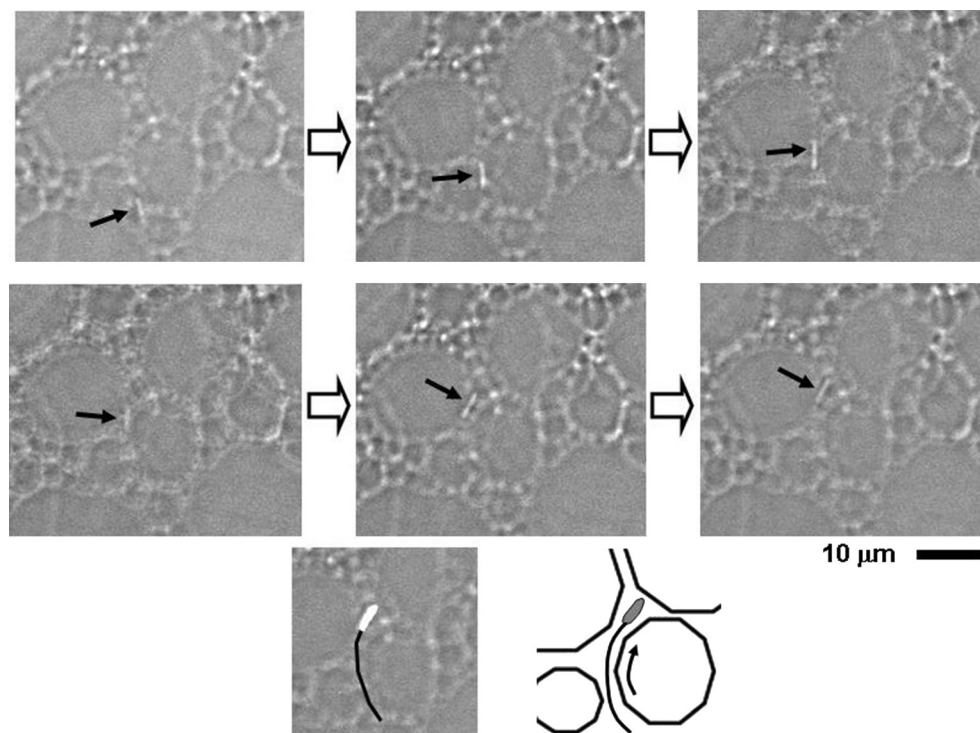


FIG. 4. Successive images showing motion of a bacterium as it secretes a cellulose nanofiber, using real-time video analysis. The bacterium was selectively attached to the honeycomb frame and synthesized its cellulose fiber on the molecular tracks on the honeycomb frame. The interval of each image was set to be 1 min.

cellulose nanofibers. When the molecular orientation on the film surface exhibits amphiphilic molecular tracks similar to those on NOC, the bacterial cells autonomously fabricate 3D honeycomb structures by deposition of secreted cellulose nanofibers on templates (5–7). According to the detailed examination for NOC, the hydrophobic phases due to the anhydroglucose plane appear alternately next to the hydrophilic OH tracks, resulting in unique amphiphilic molecular tracks. This molecular orders in the surface of the honeycomb frames appeared to have a similar ordering to NOC including molecular orientation along the honeycomb frame and tilted angle of the glucose plane (3,4,6).

The first step is to induce the bacteria to selectively secrete nanofibers onto the honeycomb frame surfaces. The bacteria were therefore incubated under slow rotation to enable the bacteria to secrete and deposit cellulose nanofibers on the surfaces of the honeycomb frames. This means that once bacteria apparently attach to the honeycomb frame surface, they keep secreting or producing nanocellulose onto the same honeycomb frame surface. In this critical rotation culture, bacteria were naturally to be selected to deposit the nanofiber onto honeycomb frames in the entire template. As a result of this selective attachment of bacterial nanofibers, which does not indicate bacterial attachment, during incubation, the cultured bacteria continuously deposit cellulose nanofibers along the honeycomb frame surfaces. Then the selective deposition was found by the real-time video observation to occur in the entire areas of honeycomb frame surfaces. Namely, this rotational culturing of the bacteria successfully achieved preferential location onto the entire honeycomb frame surface, presumably by anchoring as a result of selective interactions between the secreted nanofibers and the surfaces, as shown in Fig. 3. It should be added that before anchoring the bacterial cells were just floating and not observable in the same frame for Fig. 3.

After attached movement of *G. xylinus* along the honeycomb frame surfaces, the bacterial cells began to synthesize cellulose nanofibers, enabling further selective movements along the

honeycomb frames of the substrate, as shown in Fig. 4. In contrast, there were no cellulose fibers inside the pore spaces. The bacterial movement was therefore only regulated on the surfaces of the honeycomb frames across the entire template, as shown by direct video imaging of the motion of a bacterium as it secreted the cellulose nanofibers, as shown in Fig. 4. Presumably, the rest bacteria, which were not attached to the honeycomb frame, were floating in the media, and not capable of fixing themselves into any scaffold.

Another method of fabricating 3D honeycomb cellulose structures was reported by Nemoto et al. (12) and Uraki et al. (13). The honeycomb film was prepared by a transcription method (12), for use as a honeycomb groove for *G. xylinus* movement to give a 3D architecture. This method was based on physical mechanical control of the bacterial movements; this is totally different from the present study, which was based on physicochemical interfacial interactions between cellulose nanofibers and templates.

According to our previous report (5), the bacteria followed the orientation direction of the NOC and moved at  $4.5 \mu\text{m}/\text{min}$  at  $24^\circ\text{C}$ . In the present study, the cells moved at a constant rate of  $2.79 \pm 0.46 \mu\text{m}/\text{min}$  at  $24^\circ\text{C}$  when forming the first layer on the top of the honeycomb frame. This was considered to be the result of interactive forces between the surface of the honeycomb film and the secreted microbial cellulose fibers. For the second and subsequent layers, interactions between the cellulose nanofibers contributed to the movement rate; it became  $2.92 \pm 0.26 \mu\text{m}/\text{min}$  at  $24^\circ\text{C}$ , which was faster than that for the first layer. The experimental results could be achieved by keeping observation of bacterial deposition all through the beginning to the end under an optical microscope using real-time video system (3 frames/min). Furthermore, both rates are faster than that of  $2.0 \mu\text{m}/\text{min}$  at  $25^\circ\text{C}$  (1) for cell movement without templates. The increase in the movement rate for NOC and honeycomb templates may be caused by inhibition of self-assembly of the nascent cellulose microfibrils by the strong interactions between the biosynthesized fibers and the template (14). The increase in the number of contact points on

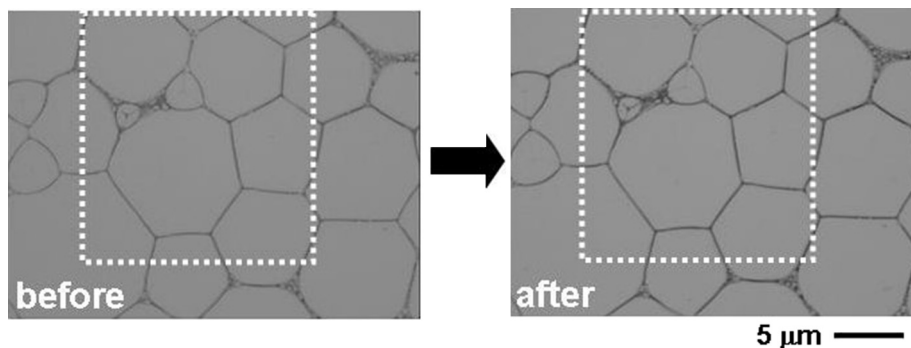


FIG. 5. Micrographs of honeycomb-patterned cellulose films before and after rotational culture. The 2D structures of the honeycomb-patterned cellulose films exhibited no change after culture.

the microfibrils then causes strong interactions with the scaffold surface. This phenomenon is the rate-determining step for both production of fibers and bacterial movement (7,14). In this case, the strong interfacial contact with the template prevented the assembly of individual cellulose microfibrils of width 3.5 nm soon after biosynthesis, resulting in an increase in the rate, and could also cause stress release in the enzymatic synthesis of cellulose (7). As a result, the production rate of fibers on the surface of an NOC-like template increases with increasing rate of bacterial movement.

Fig. 5 shows microscopic two-dimensional (2D) images of the honeycomb frames before and after incubation of the bacteria. There was no change in the 2D honeycomb pattern after culture. However, AFM observations revealed the phenomenon shown in Fig. 6. In this study, an AFM with a voice coil motor was used to obtain topographic images with very rough surfaces. Normal AFM instruments equipped with a piezoelectric scanner could not be used to observe such rough honeycomb frames, because the piezo element cannot scan the large height changes. The changes in the heights in the surface topographic images of a honeycomb-patterned cellulose film are shown in Fig. 6. Before and after incubation, microscopic observations with a light microscope and AFM were performed for the same sample, the same position, and the same measurement spot. It should be noted that great skill was needed to perform the experiments. This method was used to prove

the 2D deformation of the honeycomb pattern already shown in Fig. 5. There was no apparent change, as seen in the same figure. However, the cross-sectional AFM image (right) after incubation of the bacterial cells, shown in Fig. 6, clearly showed an increase in only the height direction of the honeycomb frames. In culture for 10 h, the average height increased by 70 nm, as shown in the height image at the bottom right of Fig. 6. If the thickness of the individual microbial cellulose microfibrils is assumed to be 3.5 nm (7), 20 layers of fibers were accumulated. It should be noted that we kept observing bacterial deposition all through the beginning to the end under an optical microscope using time lapse video system (3 frames/min). Soon after the optical observation, the height was measured in the same location of the honeycomb frame. Therefore, the substance accumulated on the honeycomb frame should be cellulose nanofibers secreted by the bacteria. These results indicate that the honeycomb pattern could be used as a template for autonomous building up of 3D structures from 2D structures, with cellulose nanofibers as the building blocks, using a bacterial nanoengine.

In summary, the molecular order of a honeycomb-patterned template was formed by stretching during natural drying stretching, resulting in characteristics similar to those of NOC (2–4). The honeycomb surface also induced epitaxial deposition of cellulose nanofibers secreted by *G. xylinus*. In this study, we clarified similar

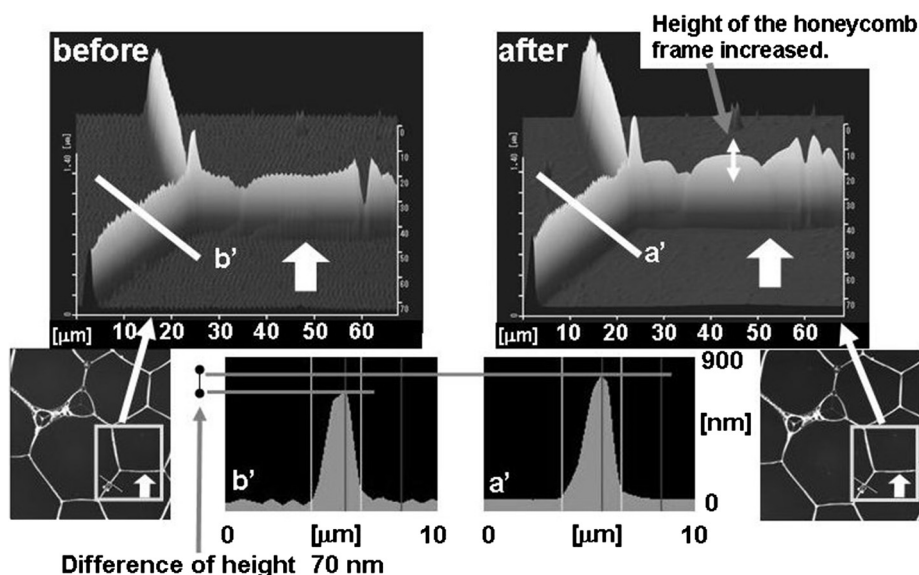


FIG. 6. Morphological changes in honeycomb frame in film, observed using atomic force microscopy, after culture. The square areas were focused and cross-sectioned, and show the 3D images before and after culture. Twenty layers of bacterial cellulose nanofibers were accumulated in 10 h (one layer = 3.5 nm).

directed deposition of secreted cellulose nanofibers on the surface of a honeycomb frame fabricated by strong interfacial interactions, leading to autonomous bottom-up fabrication of 3D nano/micro-cellulose structures. The goal of this study was to develop a method for creating novel 3D nanostructures using biological systems combined with templates with specific molecular orientation patterns.

We expect that the relationship between directed biosynthesis by bacteria and ordered fabrication from the nano- to the micro-scale will lead to sustainable bottom-up methods for the design of functional materials with desired nanostructures, with low energy consumption.

#### ACKNOWLEDGMENTS

We would like to thank Prof. R. Malcolm Brown, Jr. at the University of Texas at Austin for valuable comments. We thank Mr. T. Mitsunaga and Ms. A. Takase of the X-ray Research Laboratory, Rigaku Corporation for advice on X-ray diffractometry. Dr. W. Kasai is partly supported by a Research Fellowships of the Japan Society for the Promotion of Science for Young Scientists. This study is also partially supported by the MAFF Nanotechnology Project of the Agriculture, Forestry, and Fisheries Research Council, and by a Grant-in-Aid for Scientific Research (no. 14360101), the Japan Society for the Promotion of Science, Japan.

#### References

1. **Brown, R. M., Jr., Willison, J. H. M., and Richardson, C. L.:** Cellulose biosynthesis in *Acetobacter xylinum*: visualization of the site of synthesis and direct measurement of the in vivo process, *Proc. Natl. Acad. Sci. USA*, **73**, 4565–4569 (1976).
2. **Togawa, E. and Kondo, T.:** Change of morphological properties in drawing water-swollen cellulose films prepared from organic solutions: a view of molecular orientation in the drawing process-, *J. Polym. Sci. B: Polym. Phys.*, **37**, 451–459 (1999).
3. **Kondo, T., Togawa, E., and Brown, R. M., Jr.:** "Nematic ordered cellulose": a concept of glucan chain association, *Biomacromolecules*, **2**, 1324–1330 (2001).
4. **Kondo, T.:** Nematic ordered cellulose: its structure and properties, pp. 285–306, in: Brown, R. M., Jr. and Saxena, I. M. (Eds.), *Cellulose: molecular and structural biology*. Springer, Dordrecht (2007).
5. **Kondo, T., Nojiri, M., Hishikawa, Y., Togawa, E., Romanovicz, D., and Brown, R. M., Jr.:** Biodirected epitaxial nanodeposition of polymers on oriented macromolecular templates, *Proc. Natl. Acad. Sci. USA*, **99**, 14008–14013 (2002).
6. **Kondo, T.:** Nematic ordered cellulose templates, pp. 113–142, in: Gama, M., Gatenholm, P., and Klemm, D. (Eds.), *Bacterial nanocellulose: a sophisticated multifunctional material*. CRC Press, New York (2012).
7. **Kondo, T., Kasai, W., Nojiri, M., Hishikawa, Y., Togawa, E., Romanovicz, D., and Brown, R. M., Jr.:** Regulated patterns of bacterial cellulose templates based on their secreted cellulose nanofibers interacting interfacially with ordered chitin templates, *J. Biosci. Bioeng.*, **114**, 113–120 (2012).
8. **Higashi, K. and Kondo, T.:** Nematic ordered cellulose templates mediating order-patterned deposition accompanied with synthesis of calcium phosphates, *Cellulose*, **19**, 81–90 (2012).
9. **Kasai, W. and Kondo, T.:** Fabrication of honeycomb-patterned cellulose films, *Macromol. Biosci.*, **4**, 17–21 (2004).
10. **Hestrin, S. and Schramm, M.:** Synthesis of cellulose by *Acetobacter xylinum*. 2. Preparation of freeze dried cells capable of polymerizing glucose to cellulose, *Biochem. J.*, **58**, 345–352 (1954).
11. **Kondo, T., Kasai, W., and Brown, R. M., Jr.:** Formation of nematic ordered cellulose and chitin, *Cellulose*, **11**, 463–474 (2004).
12. **Nemoto, J., Uraki, Y., Kishikoto, T., Sano, Y., Funada, R., Obata, N., Yabu, H., Tanaka, M., and Shimomura, M.:** Production of mesoscopically patterned cellulose film, *Bioresour. Technol.*, **96**, 1955–1958 (2005).
13. **Uraki, Y., Nemoto, J., Otsuka, H., Tamai, Y., Sugiyama, J., Kishikoto, T., Ubukata, M., Yabu, H., Tanaka, M., and Shimomura, M.:** Honeycomb-like architecture produced by living bacteria, *Gluconacetobacter xylinus*, *Carbohydr. Polym.*, **69**, 1–6 (2007).
14. **Tomita, Y. and Kondo, T.:** Influential factors to enhance the moving rate of *Gluconacetobacter xylinus* due to its nanofiber secretion on oriented templates, *Carbohydr. Polym.*, **77**, 754–759 (2009).